Searching for the 21 cm Global Signal

Martin Bucher, APC, Université Paris Cité

and

The REACH Collaboration (Eloy de Lera Acedo, Dirk de Villiers Co-PIs et al.)

Triangular Conference
Univesity of Edinburgh, 21 April 2024

Outline

1. What is the global 21 cm signal? Why is it interesting?
2. What has been claimed?
3. Techniques for measuring the CMB
4. Making Absolute Measurements of Spectral Distortions of the Extreme Rayleigh-Jeans Tail of the CMB
5. Calibration, Amplifiers and Noise

FIRAS Determination of Frequency Spectrum

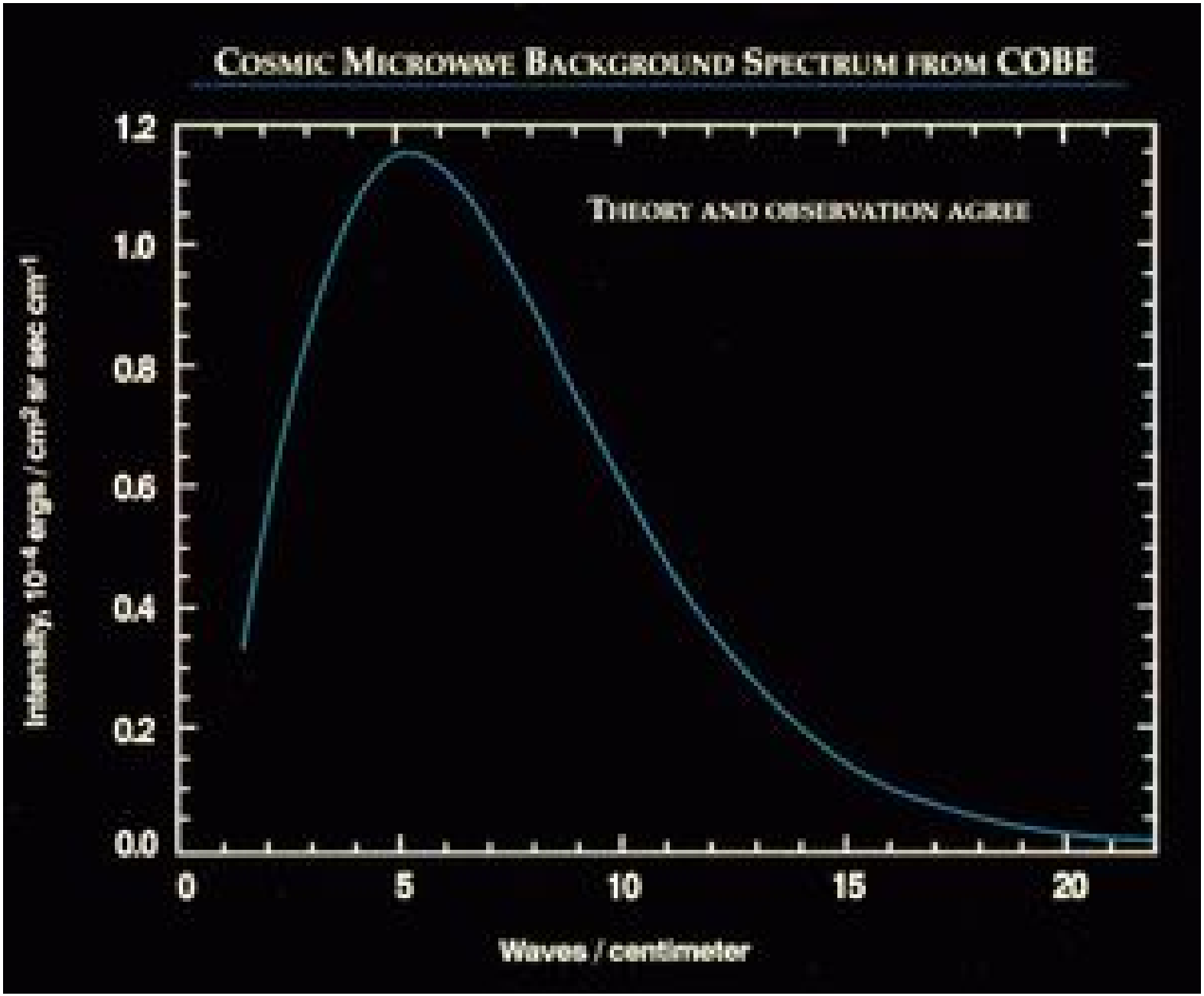

Microwave Foreground Frequency Spectra

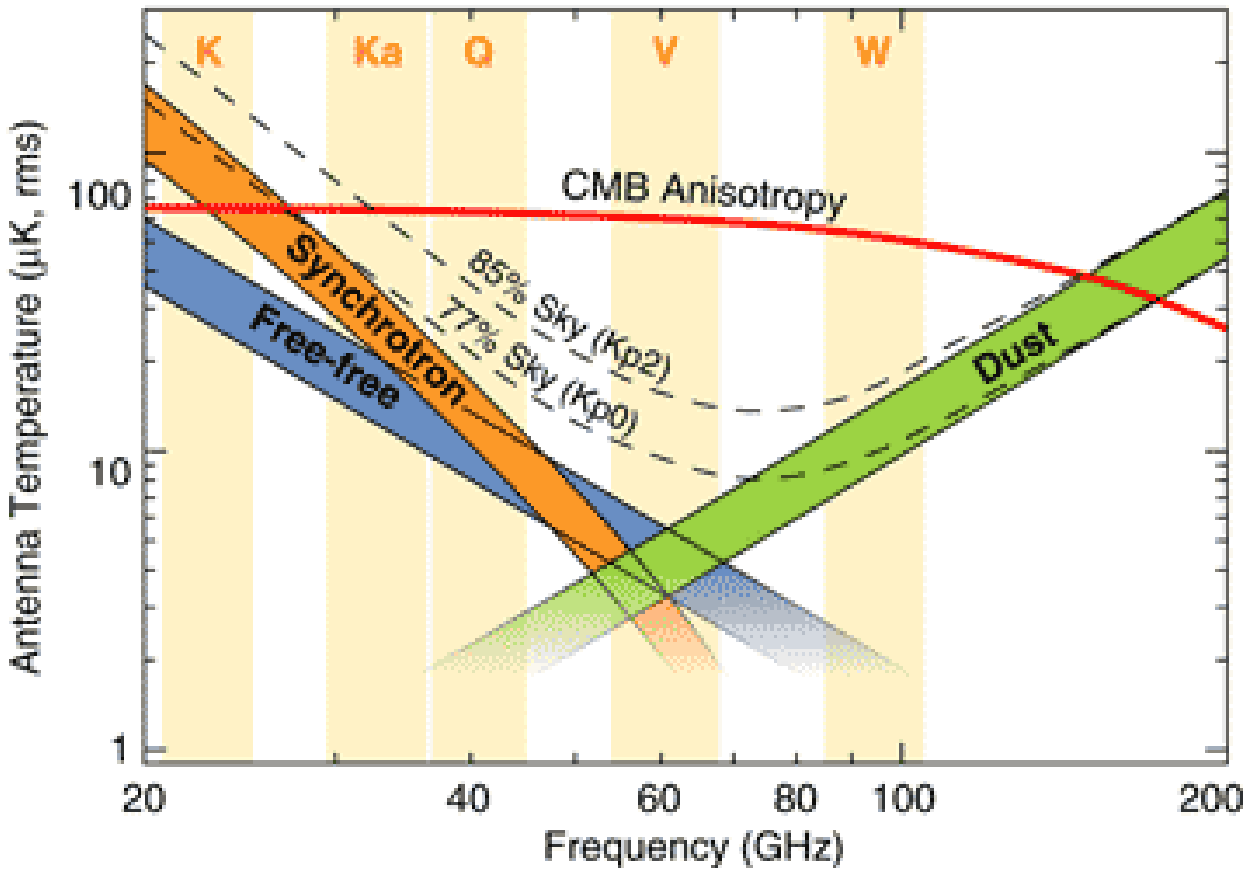

There is a narrow window in frequency ranging from around 40 GHz to 150 GHz within which the CMB anisotropies dominate over other astrophysical foreground components.

21 cm Hyperfine Transition – Atomic Hydrogen (HI)

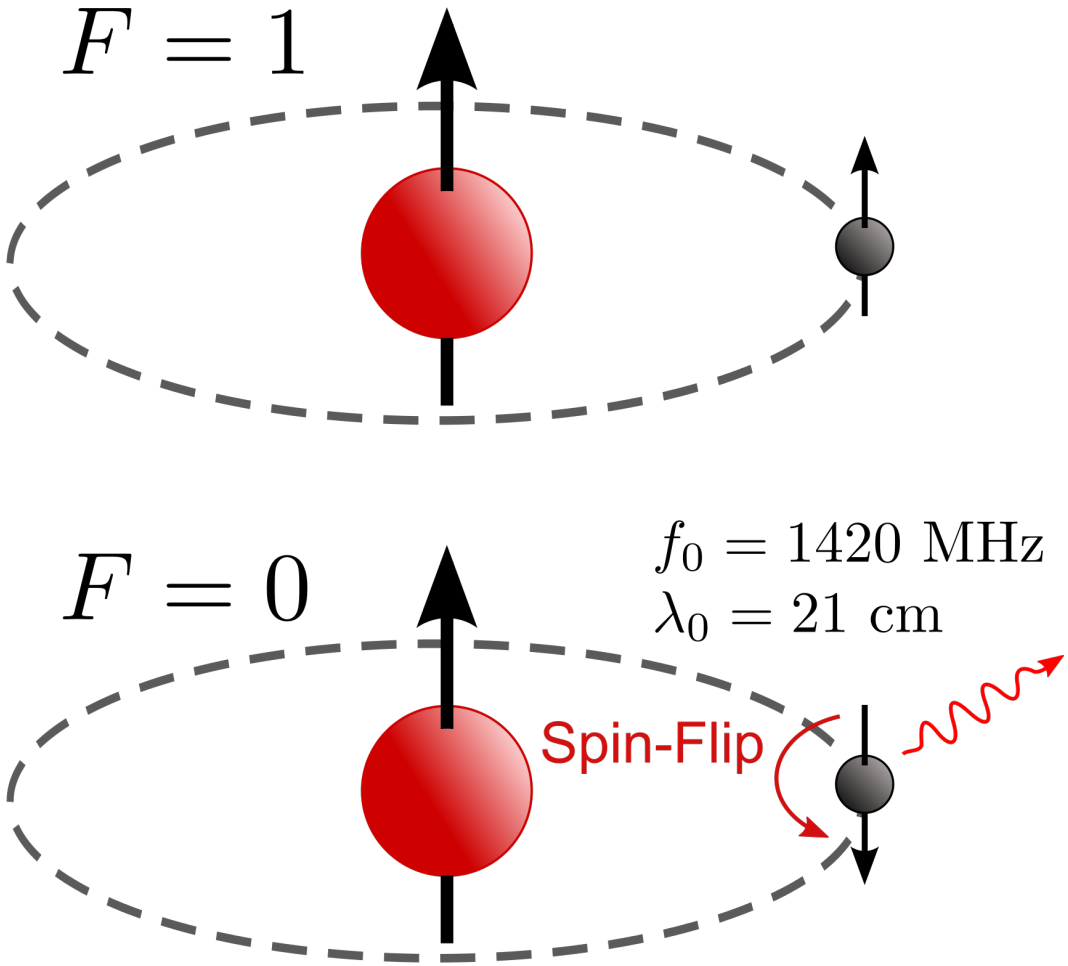

21 cm Distortions of the Low Frequency CMB Spectrum

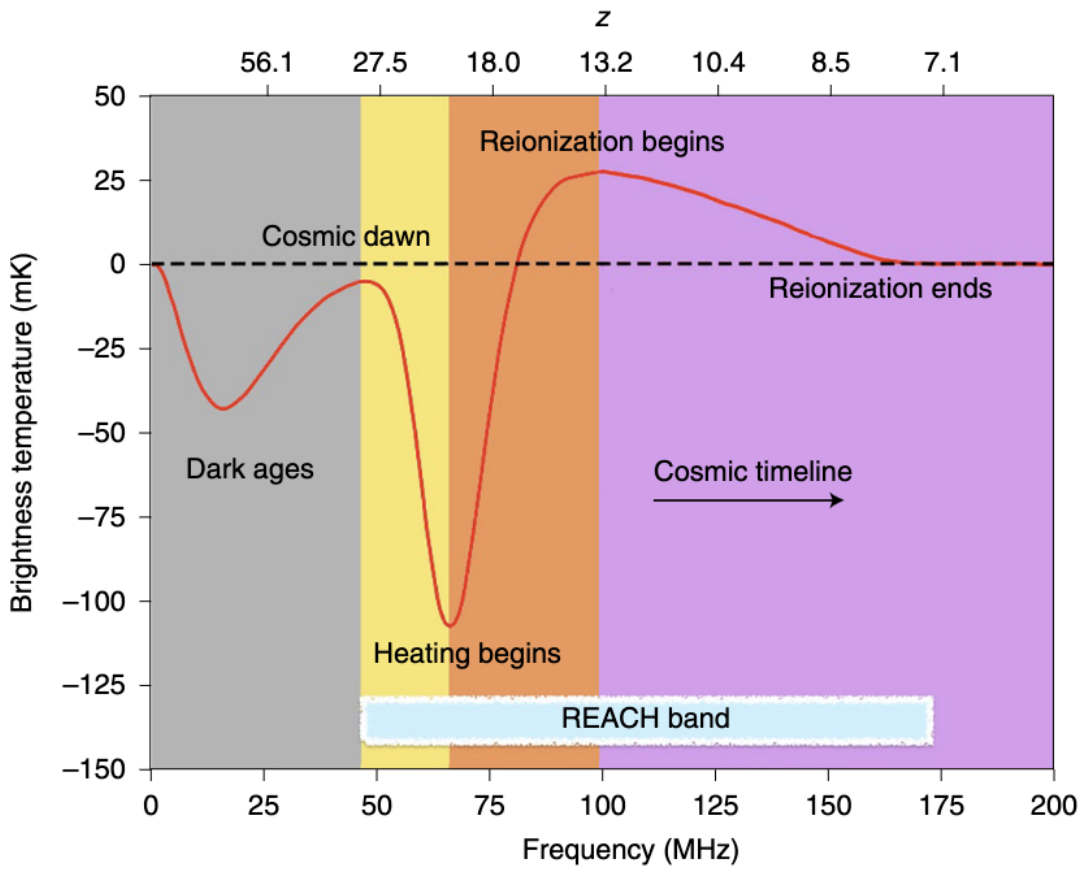

Fig. 1 | A typical model of the global 21-cm line. Main cosmic events are highlighted[23,24]. From left to right: collisional coupling (grey), onset of Ly-α coupling (yellow), onset of X-ray heating (orange), photoionization (purple). REACH will explore the frequency range 50–170 MHz ($z \approx 7.5$–28).

Wouthuysen-Field Effect (simplified)

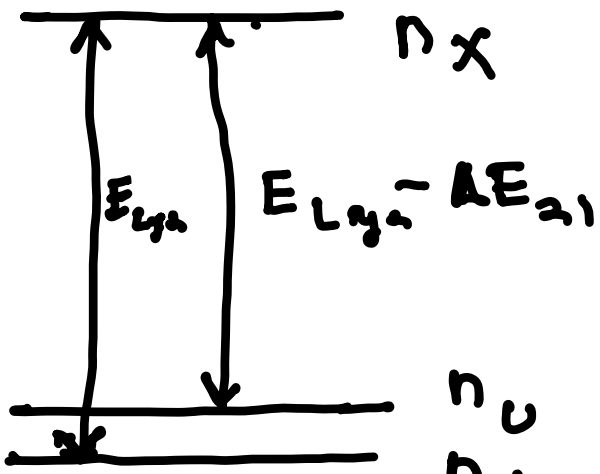

$$\dot{n}_X = -A_{X} + A\left(n_U N_E + n_L U_{E+\Delta E}\right)$$

$$\dot{n}_U = +\frac{A}{2} n_X - A\, n_U\, N_E$$

$$\dot{n}_L = +\frac{A}{2} n_X - A\, n_L\, N_{E+\Delta E}$$

$$\dot{n}_X = \dot{n}_U = \dot{n}_L = 0 \Rightarrow n_U N_E = n_L N_{E+\Delta E}$$

$$\frac{n_U}{n_L} = \frac{N_{E+\Delta E}}{N_E} = e^{-\Delta E_{21} / T_S}$$

(Same for Doppler splitting)

THE CLAIM

An absorption profile centred at 78 megahertz in the sky-averaged spectrum

Judd D. Bowman, Alan E. E. Rogers, Raul A. Monsalve, Thomas J. Mozdzen & Nivedita Mahesh

Nature **555**, 67–70 (2018) | Cite this article

39k Accesses | **780** Citations | **2135** Altmetric | Metrics

Abstract

After stars formed in the early Universe, their ultraviolet light is expected, eventually, to have penetrated the primordial hydrogen gas and altered the excitation state of its 21-centimetre hyperfine line. This alteration would cause the gas to absorb photons from the cosmic microwave background, producing a spectral distortion that should be observable today at radio frequencies of less than 200 megahertz[1]. Here we report the detection of a flattened absorption profile in the sky-averaged radio spectrum, which is centred at a frequency of 78 megahertz and has a best-fitting full-width at half-maximum of 19 megahertz and an amplitude of 0.5 kelvin. The profile is largely consistent with expectations for the 21-centimetre signal induced by early stars; however, the best-fitting amplitude of the profile is more than a factor of two greater than the largest predictions[2]. This discrepancy suggests that either the primordial gas was much colder than expected or the background radiation temperature was hotter than expected. Astrophysical phenomena (such as radiation from stars and stellar remnants) are unlikely to account for this discrepancy; of the proposed extensions to the standard model of cosmology and particle physics, only cooling of the gas as a result of interactions between dark matter and baryons seems to explain the observed amplitude[3]. The low-frequency edge of the observed profile indicates that stars existed and had produced a background of Lyman-α photons by 180 million years after the Big Bang. The high-frequency edge indicates that the gas was heated to above the radiation temperature less than 100 million years later.

EDGES Antenna

Edges Results (Nature 2018)

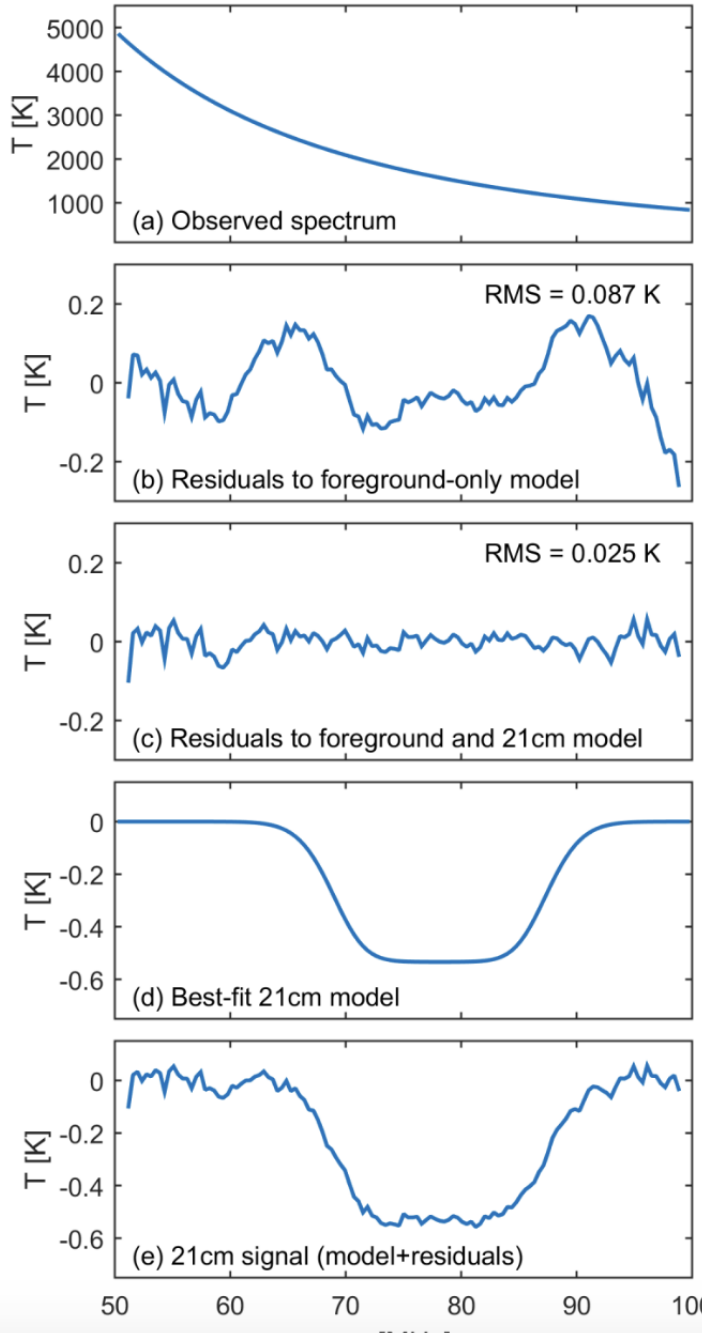

Range of Global 21cm Predictions (Cohen, Fialkov & Barkana, 2018)

The chosen curve teaches us about the first stars and quasars

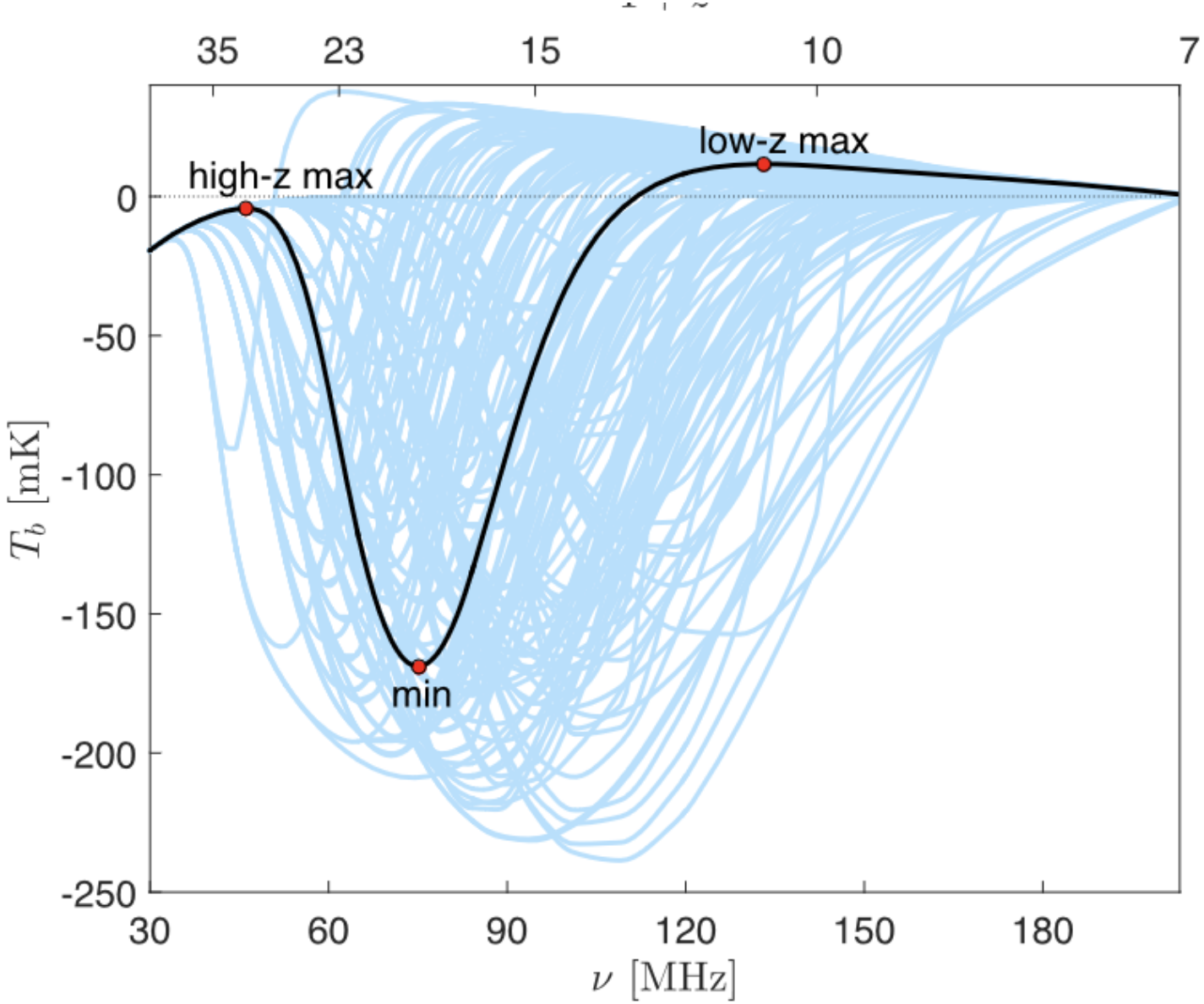

Global 21cm Experiments

Table 1 | Comparison of main experimental features of existing global experiments with REACH

Experiment	Bandwidth	Frequency band (MHz)	Simultaneous observations	Antenna type	Receiver calibrator and spectrometer	Full Bayesian analysis
EDGES	2:1	50–100 (Low band), 100–200 (High band)	No	Blade dipole	Lab measurements, auto-correlation	No
SARAS	5:1	40–200 (SARAS2)	No	Monopole	Lab measurements, cross-correlation	No
LEDA	2.125:1	30–85	No	Crossed drooping dipole	Lab measurements, auto-correlation	No
PRIZM	2:1	50–90, 70–140	No	Crossed-dipole (four-square)	Lab measurements, auto-correlation	No
SCI-H I	3.21:1	40–130	No	HIBiscus	Lab measurements, auto-correlation	No
BIGHORNS	2.85:1	70–200	No	Conical log-spiral	Lab measurements, auto-correlation	No
REACH	**3.4:1**	**50–170**	**2 antennas**	**Hexagonal dipole, Conical log-spiral**	**In-field measurements, auto-correlation**	**Yes**

MEASURING THE CMB

WMAP Differential Measurement Set-Up

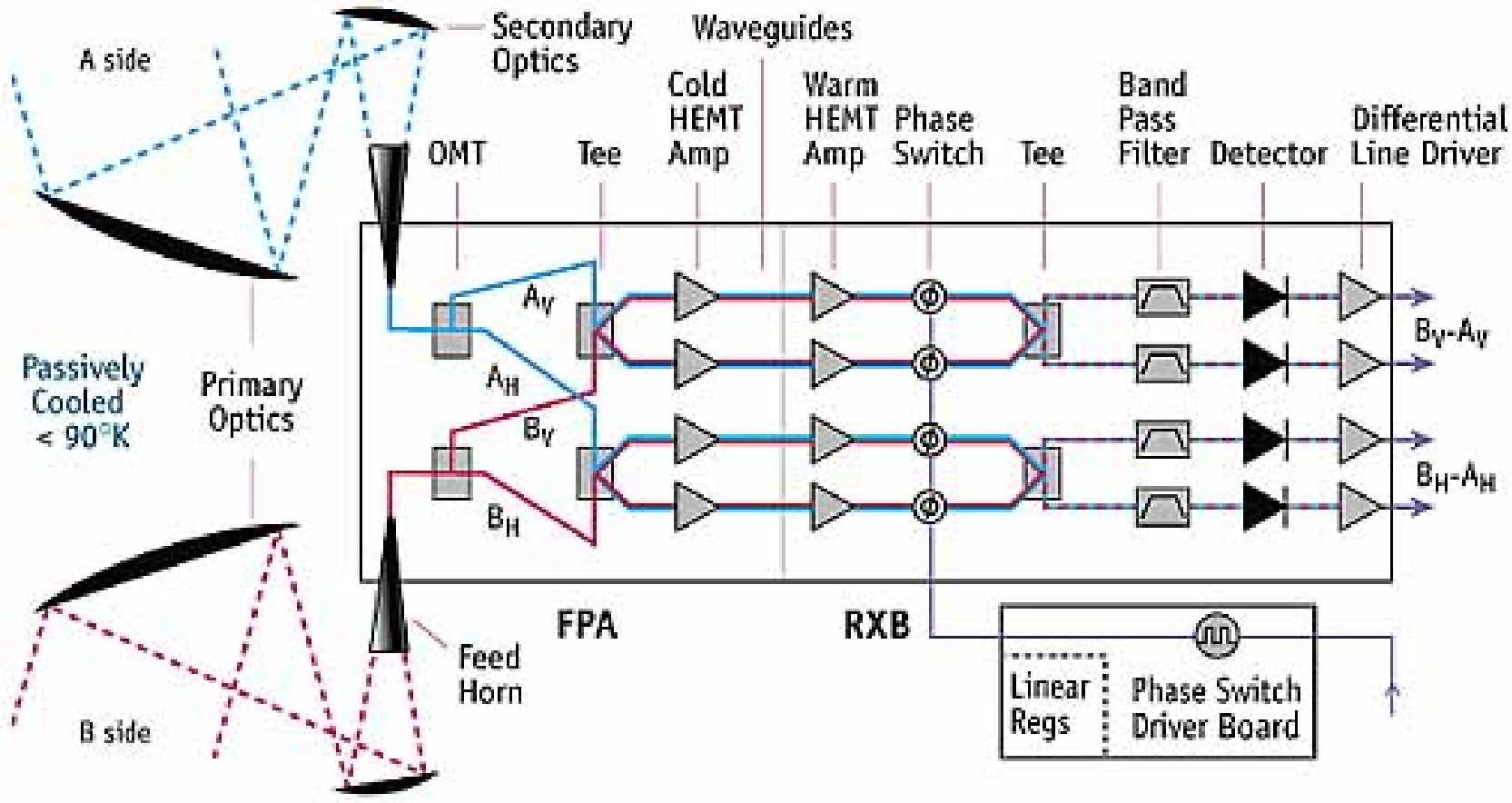

Planck bolometric detector noise power spectrum

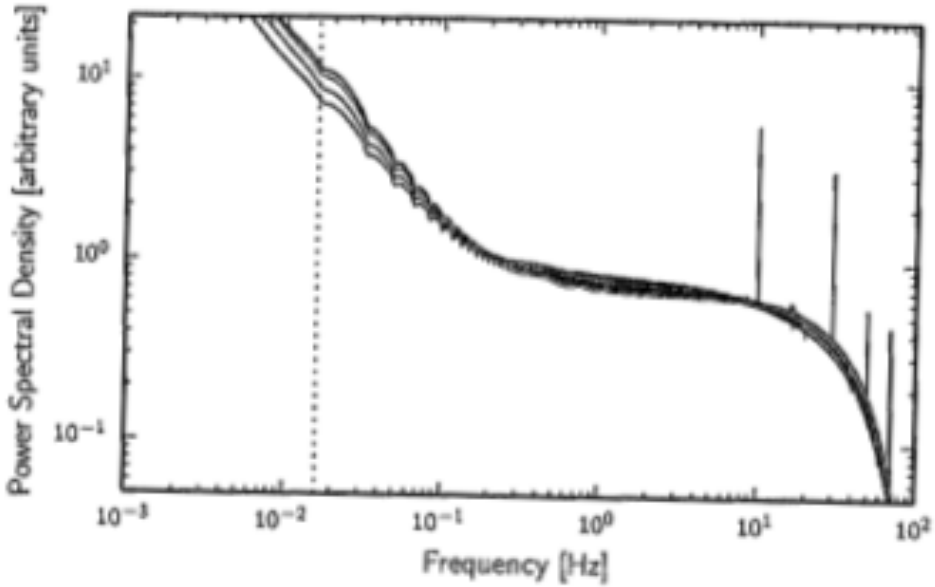

Fig. 1. The mean power spectra of the signal-subtracted time ordered data from Survey 2 for each polarization-sensitive HFI frequency channel. The spectra are normalized at 0.25 Hz. Blue, green, red, and cyan mark 100, 143, 217, and 353 GHz, respectively. The vertical dashed line shows the spacecraft spin frequency. The sharp spikes at high frequencies are the so-called 4-K cooler lines. These noise spectra are built before the time transfer function deconvolution.

Standard Ansatz for detector noise

We assume Gaussian stationary noise completely characterized by a power spectrum

$$\langle n(\nu)\ n(\nu')\rangle = N(\nu)\delta(\nu - \nu'), \tag{1}$$

and additionally the Ansatz

$$N(\nu) = N_{white}\left(1 + \left(\frac{\nu_{knee}}{\nu}\right)^{\alpha}\right]. \tag{2}$$

Typically, $1 \lesssim \alpha \lesssim 2$ and $\nu_{knee} \approx 200\ mHz$ for Planck but has been observed as small as 10 mHz in the laboratory. However, the Planck detectors tested in the lab showed comparable performance, and it is not fully understood why the performance in space was so much poorer.

The curse of low frequency excess noise

- $1/f^{\alpha}$ noise means that we cannot make absolute measurements.
- The zero point is floating and provides no meaningful information.

Mathematically, the integral

$$N(t) = 2 \int_0^{\infty} d\nu \; N(\nu) \; \cos(2\pi\nu t) \tag{3}$$

diverges for $\alpha \geq 0$.

- Only differences of measurements taken between a short time span $t \lesssim {\nu_{knee}}^{-1}$ contribute meaningful information.

The curse of $1/f$ noise is not new

- In 1947 Dicke proposed switching between different points in the sky or between the sky and a cold source to eliminate $1/f$ noise in the microwave amplifiers/detector available at the time.
- COBE and WMAP had pairs of horns or telescope, respectively, and only the differences were used, so that the noise of the data stream was more or less "white". Planck LFI did more or less the same but with an artificial load. HEMTs must be switched at $\approx (\mathrm{few})\ \mathrm{kHz}$ is order to control low frequency excess noise.
- Old map making is simple—essentially least squares—whereas modern map making would not be possible without fast computers. Implicit differencing in software replaces differences implemented in hardware.

Spin-precession family of scanning strategies

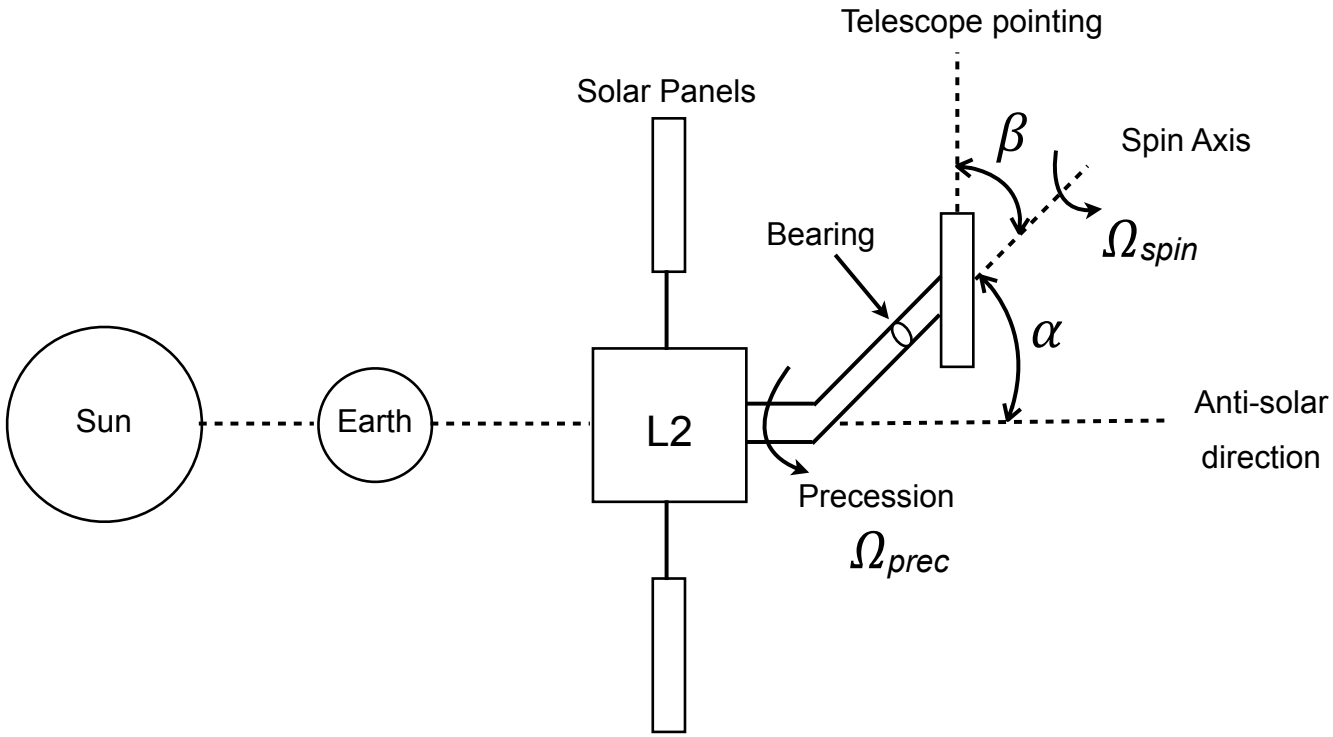

Pattern on sky

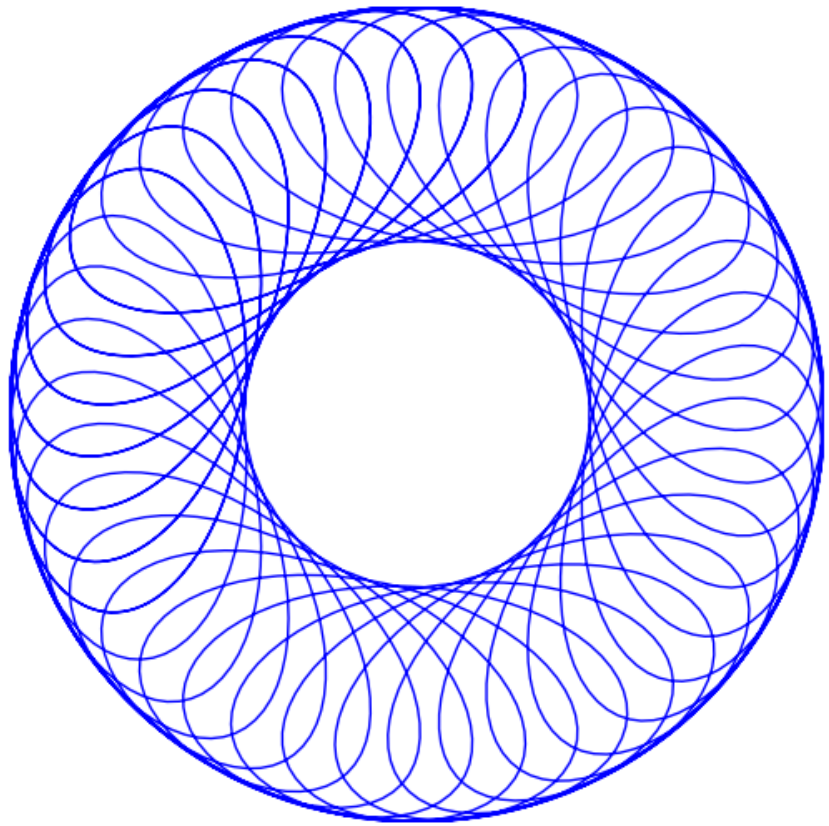

This pattern is centered on the ecliptic equator and precesses around over the course of the year.

The map making equation (easy to write, harder to solve for big maps)

The underlying (approximate) statistical model

$$\mathbf{d} = \mathbf{A}\ \mathbf{m} + \mathbf{n} \tag{4}$$

$$\mathbf{d} \equiv (\text{vector of data taken})$$

$$\mathbf{m} \equiv (\text{true sky map})$$

$$\mathbf{A} \equiv (\text{pointing matrix})$$

$$\mathbf{n} \equiv (\text{noise vector})$$

$$\mathbf{N} \equiv (\text{detector noise covariance matrix})$$

The **maximum likelihood sky map** is given by

$$\mathbf{m}_{ML} = (\mathbf{A}^T\mathbf{N}^{-1}\mathbf{A})^{-1}(\mathbf{A}^T\mathbf{N}^{-1})\mathbf{d} \tag{5}$$

The map making filter $N^{-1}(t)$

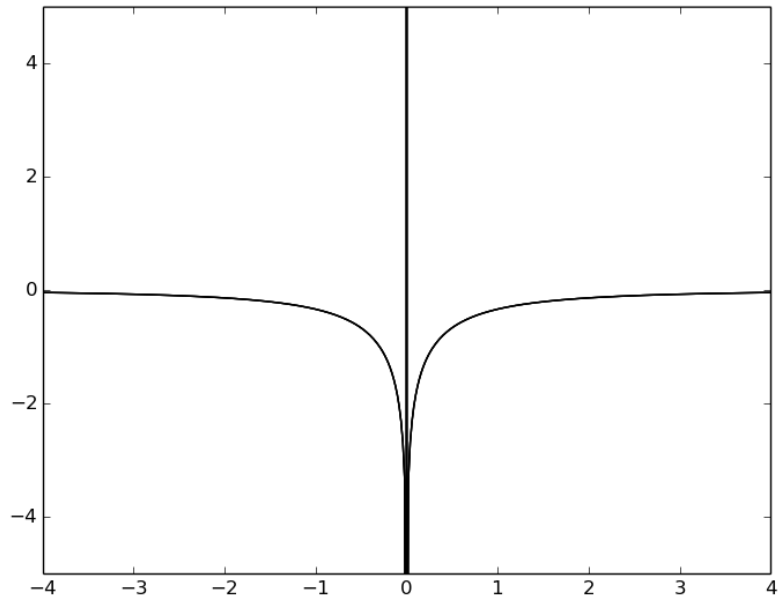

$$
\begin{aligned}
N^{-1}(t) &= 2\int_0^\infty d\nu\ N^{-1}(\nu)\ \cos(2\pi\nu t) \\
&= 2{N_{white}}^{-1}\int_0^\infty d\nu\ \left(\frac{\nu}{\nu+\nu_{knee}}\right)\ \cos(2\pi\nu t), \qquad (6)
\end{aligned}
$$

This is a high pass filter. The $\nu = 0$ is completely blocked. The constant offset and linear drifts are removed from the data stream because they carry no useful information.

FIRAS Determination of Frequency Spectrum

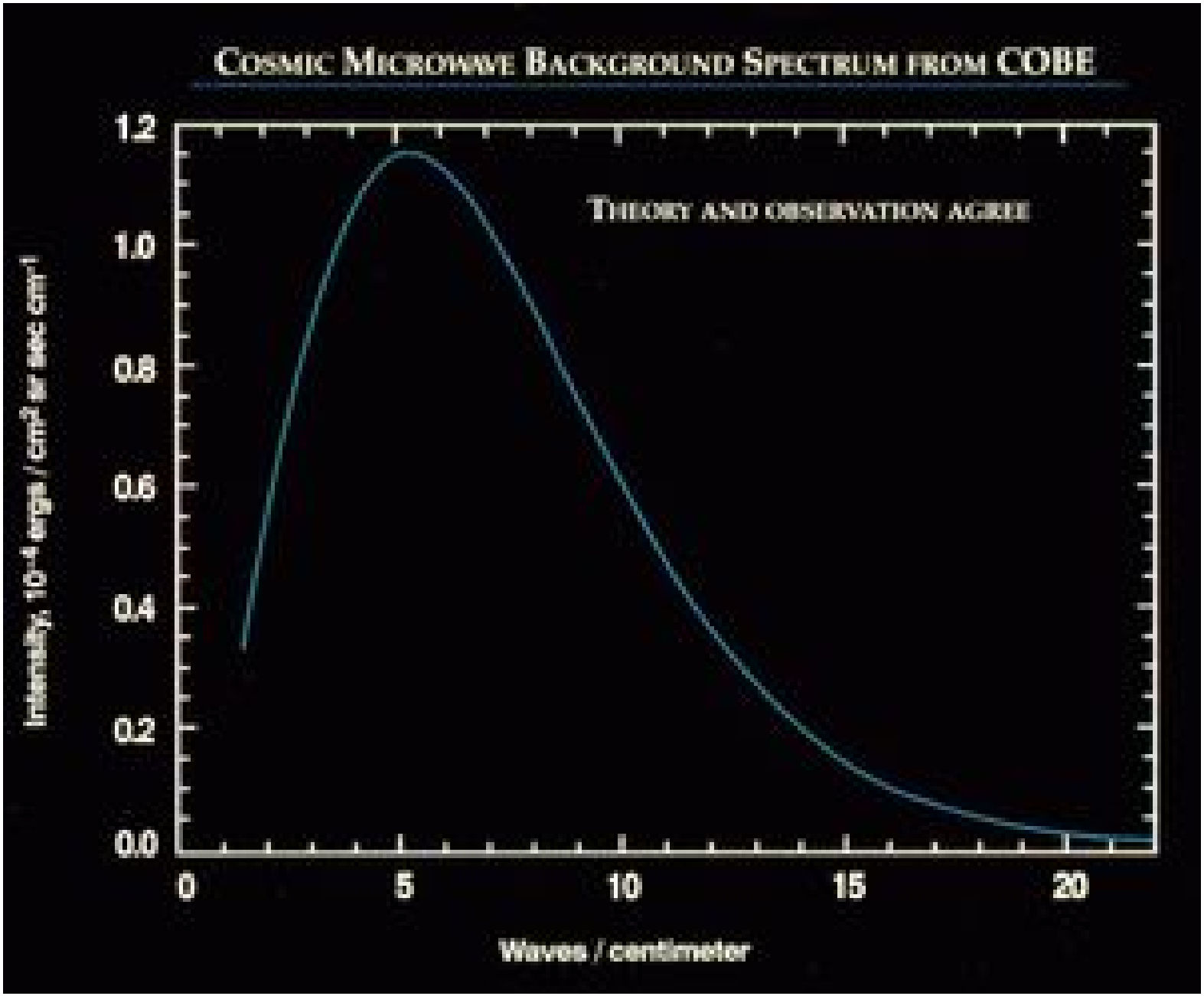

PIXIE Block Diagram (after FIRAS)

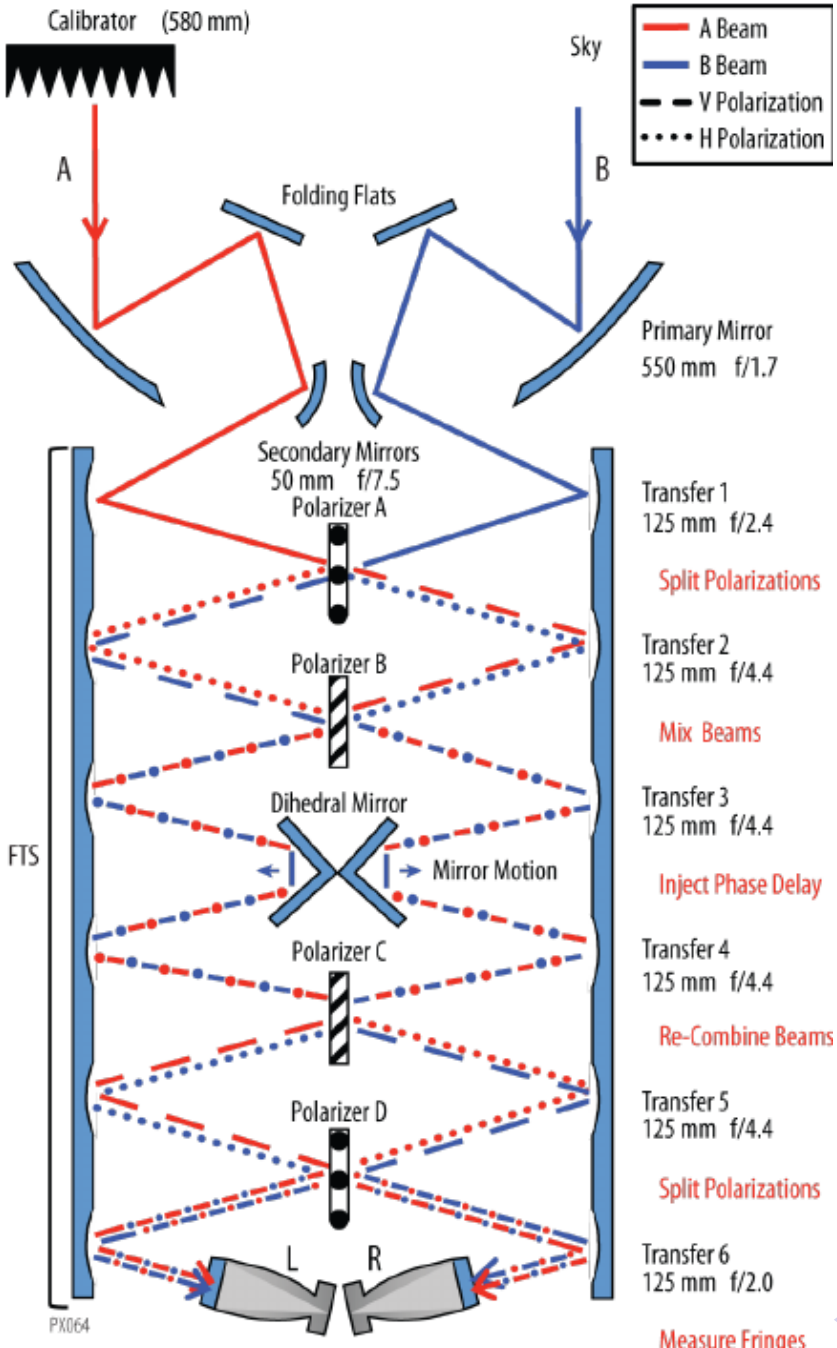

A more perfect blackbody...

THE REACH EXPERIMENT

nature astronomy

ARTICLES

https://doi.org/10.1038/s41550-022-01709-9

Check for updates

The REACH radiometer for detecting the 21-cm hydrogen signal from redshift $z \approx 7.5$–28

E. de Lera Acedo[1,2]✉, D. I. L. de Villiers[3], N. Razavi-Ghods[1], W. Handley[1,2], A. Fialkov[2,4], A. Magro[5], D. Anstey[1], H. T. J. Bevins[1], R. Chiello[6], J. Cumner[1], A. T. Josaitis[1], I. L. V. Roque[1], P. H. Sims[7,8], K. H. Scheutwinkel[1], P. Alexander[1], G. Bernardi[9,10,11], S. Carey[1], J. Cavillot[12], W. Croukamp[3], J. A. Ely[1], T. Gessey-Jones[1], Q. Gueuning[1], R. Hills[1,20], G. Kulkarni[13], R. Maiolino[1,2], P. D. Meerburg[14], S. Mittal[13], J. R. Pritchard[15], E. Puchwein[16], A. Saxena[14], E. Shen[1], O. Smirnov[10,11], M. Spinelli[17,18,19] and K. Zarb-Adami[5,6]

Observations of the 21-cm line from primordial hydrogen promise to be one of the best tools to study the early epochs of the Universe: the dark ages, the cosmic dawn and the subsequent epoch of reionization. In 2018, the Experiment to Detect the Global Epoch of Reionization Signature (EDGES) caught the attention of the cosmology community with a potential detection of an absorption feature in the sky-averaged radio spectrum centred at 78 MHz. The feature is deeper than expected, and, if confirmed, would call for new physics. However, different groups have re-analysed the EDGES data and questioned the reliability of the signal. The Radio Experiment for the Analysis of Cosmic Hydrogen (REACH) is a sky-averaged 21-cm experiment aiming at improving the current observations by tackling the issues faced by current instruments related to residual systematic signals in the data. The novel experimental approach focuses on detecting and jointly explaining these systematics together with the foregrounds and the cosmological signal using Bayesian statistics. To achieve this, REACH features simultaneous observations with two different antennas, an ultra-wideband system (redshift range about 7.5 to 28) and a receiver calibrator based on in-field measurements. Simulated observations forecast percent-level constraints on astrophysical parameters, potentially opening up a new window to the infant Universe.

The Karoo: A Radio Quiet Site

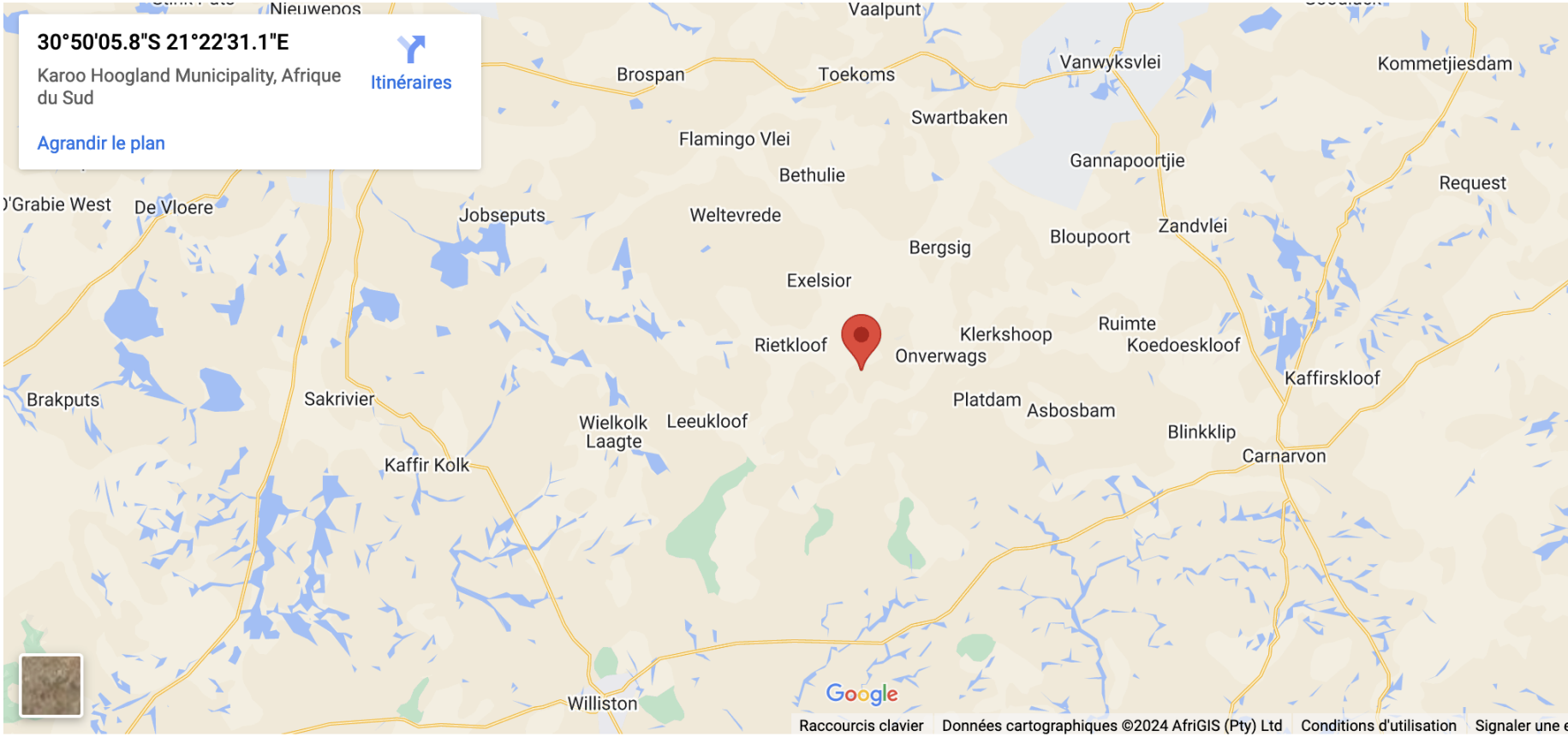

The REACH Antenna

Does this calibration work? (I)

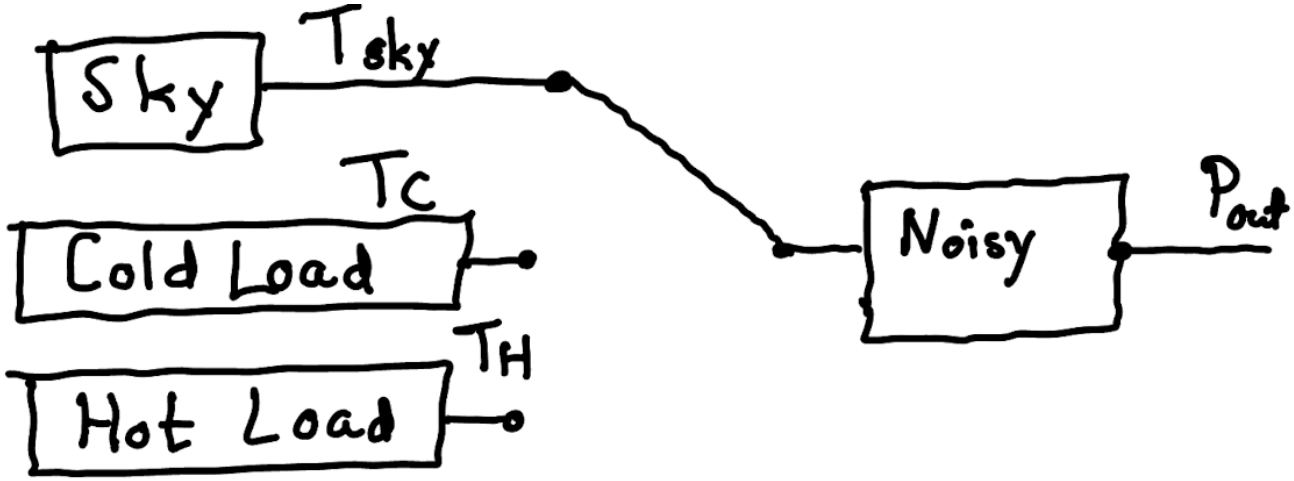

$$P_{out} = c[T_{in} + T_{noise}].$$

$$T_{ant} = T_C + \frac{T_H - T_C}{P_H - P_C}(P_{source} - P_C).$$

Does this calibration work? (II)

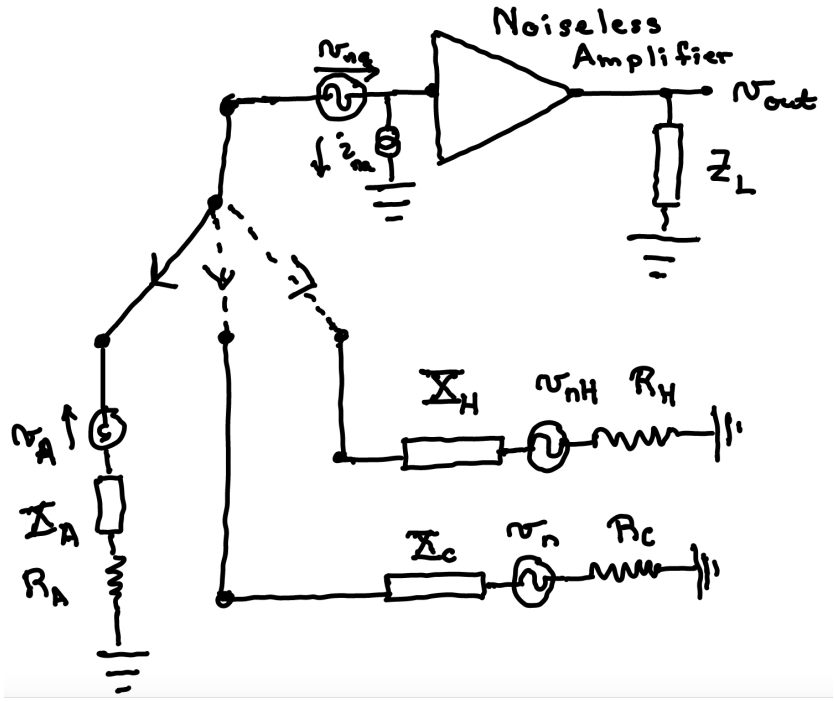

$$P_{out} = c[T_{in} + T_{noise}].$$

$$T_{ant} = T_C + \frac{T_H - T_C}{P_H - P_C}(P_{source} - P_C).$$

Schematic of REACH Calibration

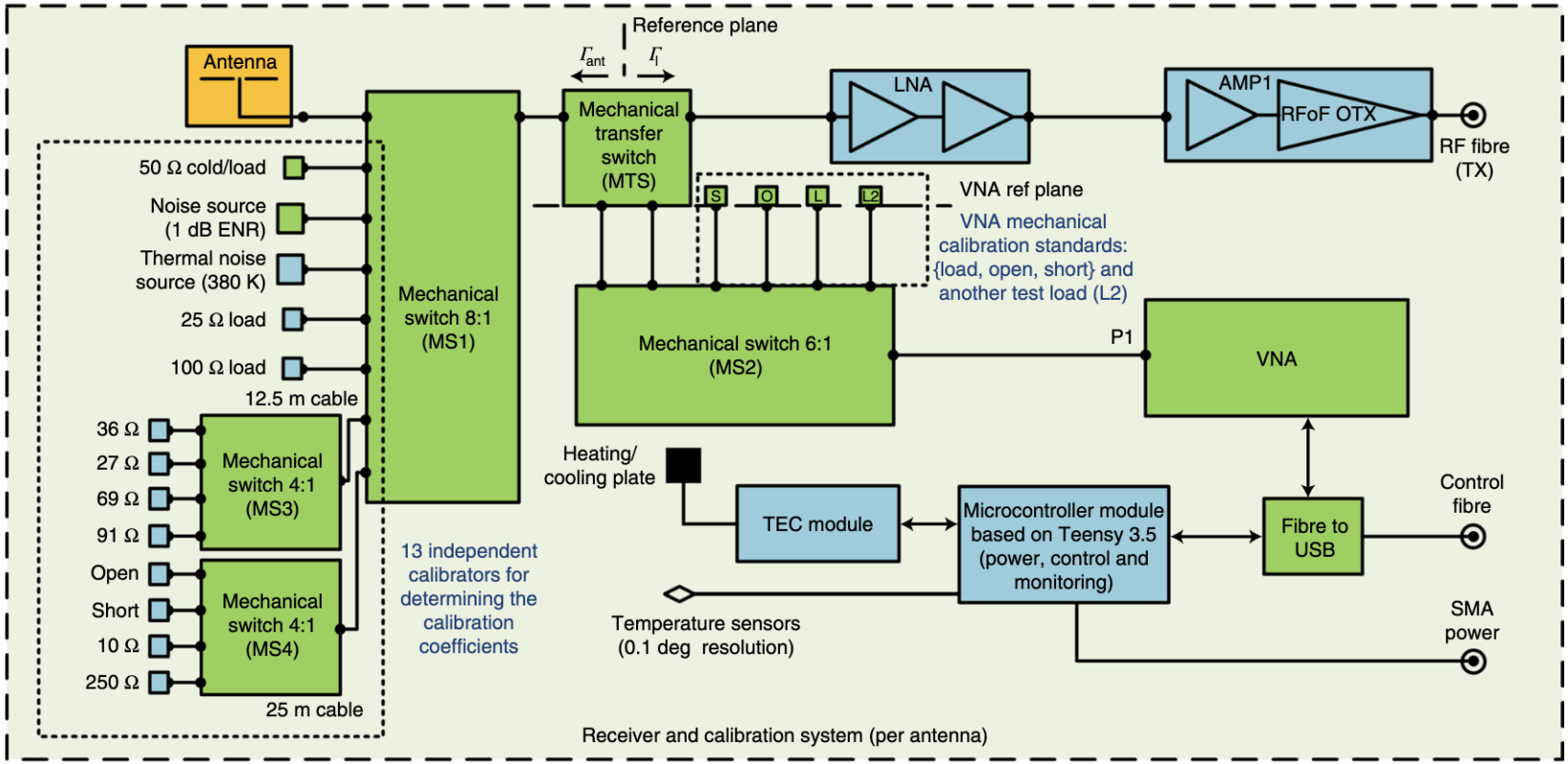

Noisy N-ports

MB & D Molnar, Representation of a Noisy Transmission Line

https://arxiv.org/abs/2404.10908 (submittted to IEEE Trans. Micro. Theory & Techniques)

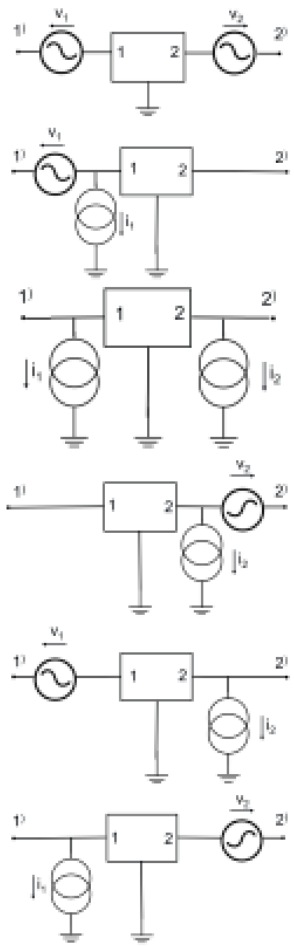

Fig. 2. Six Equivalent Noisy 2-Port Representations.

When the admittance matrix $\mathbf{Y}$ is defined, where $\mathbf{Y} = \mathbf{Z}^{-1}$ when $\mathbf{Z}$ is non-singular and invertible, we may similarly turn all voltage sources into current sources, so that

line, although a complex characteristic impedance is possible as well, and the transmission line can be fictitious.

In this travelling wave picture [10], [11], the voltage current source combination may be replaced by 'in' and 'out' travelling wave sources, as sketched in Fig. 6. Whereas in Fig. 6a the voltage and current sources impose jump conditions between v^{ext} and v^{int}, and between i^{ext} and i^{int}, respectively, in Fig. 6b the travelling wave sources impose jump conditions between $v^{in,ext}$ and $v^{in,int}$, and between $v^{out,ext}$ and $v^{out,int}$.

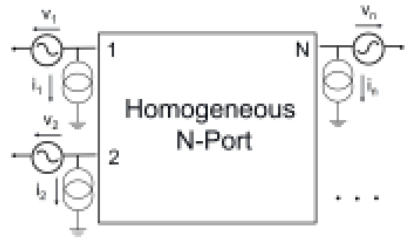

Fig. 3. General Noisy N-Port Representations.

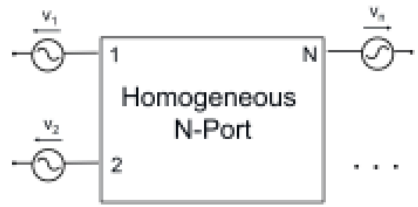

Fig. 4. Noisy N-Port Representation With Only Voltage Sources.

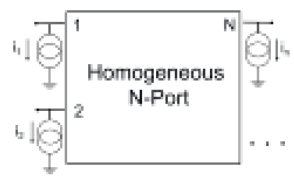

Fig. 5. Noisy N-Port Representation With Only Current Sources.

Noisy Transmission Line

MB & D Molnar, Representation of a Noisy Transmission Line

https://arxiv.org/abs/2404.10908 (submittted to IEEE Trans. Micro. Theory & Techniques)

Arbitrary temperature profile:

$$\begin{pmatrix} \langle v_{out}(L)v_{out}(L)^*\rangle & \langle v_{out}(L)i_{out}(L)^*\rangle \\ \langle i_{out}(L)v_{out}(L)^*\rangle & \langle i_{out}(L)i_{out}(L)^*\rangle \end{pmatrix} = 4k_B B \int_0^L dx\ T(x)$$

$$\times \begin{pmatrix} \cos[\bar{k}x] & jZ_c \sin[\bar{k}x] \\ j\sin[\bar{k}x]/Z_c & \cos[\bar{k}x] \end{pmatrix} \begin{pmatrix} \mathcal{R} & 0 \\ 0 & \mathcal{G} \end{pmatrix} \begin{pmatrix} \cos[\bar{k}^*x] & -j\sin[\bar{k}x^*x]/Z_c^* \\ -jZ_c^*\sin[\bar{k}^*x] & \cos[\bar{k}^*x] \end{pmatrix}$$

$$= 4k_B B \int_0^L dx\ T(x) \left[\mathcal{R} \begin{pmatrix} \cos[\bar{k}x]\cos[\bar{k}^*x] & -j\dfrac{\cos[\bar{k}x]\sin[\bar{k}^*x]}{Z_c^*} \\ +j\dfrac{\sin[\bar{k}x]\cos[\bar{k}^*x]}{Z_c} & \dfrac{\sin[\bar{k}x]\sin[\bar{k}^*x]}{Z_c Z_c^*} \end{pmatrix} \right.$$

$$\left. + \mathcal{G} \begin{pmatrix} Z_c Z_c^* \sin[\bar{k}x]\sin[\bar{k}^*x] & +jZ_c\sin[\bar{k}x]\cos[\bar{k}^*x] \\ -jZ_c^*\cos[\bar{k}x]\sin[\bar{k}^*x] & +\cos[\bar{k}x]\cos[\bar{k}^*x] \end{pmatrix} \right]$$

Constant temperature profile:

$$\begin{pmatrix} \langle v_L(L)v_L(L)^*\rangle & \langle v_L(L)v_R(L)^*\rangle \\ \langle v_R(L)v_L(L)^*\rangle & \langle v_R(L)v_R(L)^*\rangle \end{pmatrix} = \frac{4\mathcal{R}k_B T_0 B}{4\mathrm{Re}(Z_{ref})} \begin{pmatrix} \dfrac{1-\exp(-2\gamma L)}{2\gamma} & \dfrac{-j(\exp(-2jkL)-1)}{2k} \\ \dfrac{+j(\exp(+2jkL)-1)}{2k} & \dfrac{\exp(+2\gamma L)-1}{2\gamma} \end{pmatrix}$$

$$+ \frac{4\mathcal{G}k_B T_0 B\ |Z_c|^2}{4\mathrm{Re}(Z_{ref})} \begin{pmatrix} \dfrac{1-\exp(-2\gamma L)}{2\gamma} & \dfrac{-j(\exp(-2jkL)-1)}{2k} \\ \dfrac{+j(\exp(+2jkL)-1)}{2k} & \dfrac{\exp(+2\gamma L)-1}{2\gamma} \end{pmatrix}$$

Conclusions

- Mapping out the spectral distortion of the extreme Rayleigh-Jeans tail of the CMB blackbody spectrum will help constrain Cosmic Dawn and the Age of recombination.
- The global (absolute) measurement is complementary to mapping the inhomogeneities in the $(\mathbf{n}, \nu)$ cube by experiments such as HERA,....
- This measurement is difficult because of the large wavelengths involved and the lack of a relevant comparison, as is possible for FIRAS/PIXIE/....
- Modelling will be crucial to understanding what is actually being measured. The perfect achromatic antenna does not exist.
- Stay tuned....